

Turbulent Combustion Modeling Within Porous Media Using Detailed Chemical Kinetic

Bakhshan Y*, Motadayen Aval S and Abdi B

Department of Mechanical Engineering, University of Hormozgan, Iran

Abstract

In this study a CFD based code has been developed to simulate the turbulence reactive flow combustion of natural gas in a porous media. The governing equations of turbulence reactive flow in this media have been derived using space-time averaging methods. For modeling the turbulence, the macroscopic standard k- ϵ turbulence model and for combustion modeling a detailed chemical kinetic scheme has been used. The radiation heat flux from solid to gas has been considered and is calculated using the discrete ordinate method. The comparison between simulation results and experimental data show generally to have a good agreement.

Keywords: Porous burner; Turbulent; Combustion; Radiation; CFD; k- ϵ

Introduction

Turbulent flow combustion within porous media has many applications in different industries and systems, such as burners, internal combustion engines and etc. This media owing to high density burning, high dynamics power, lower pollutants emission and high burning speed has more application compare to other conventional combustion Media. In addition, to study the free flame flows, the advantages of having a combustion process inside an inert porous matrix are today well recognized [1-4]. A variety of applications of efficient radiant porous burners can be encountered in power and process industries where, it requires advanced and adequate mathematical tools in order to have a reliable design and analysis of such efficient engineering equipment.

Many researchers have worked in this field [5-15] and in the majority of their publications on combustion in porous media, the flow has been considered to remain in laminar regime. However, due to the importance of turbulence reactive flows in porous media, authors in this work developing models for turbulent flow with and without combustion. Non-Reactive turbulence flow in porous media has been studied by several researchers [16-18]. A concept called double-decomposition was proposed [16,17], in which variables were decomposed simultaneously in time and space. Also, intra-pore turbulence was accounted for all transport equations but only non-reactive flow has been investigated. Lim and Matthews [11] simulated the turbulence flow combustion with using k- ϵ model. Sahraei and Kaviani [13] have contributed a direct numerical simulation of turbulence flow in a combustion system. Delmos [17] studied the turbulence combustion in a porous burner in one-dimensional. He used a global reaction for calculation of heat release from combustion of fuel and used standard k- ϵ turbulence model in his work.

In this study, combustion of turbulence flow of natural gas and air in a porous burner which has scattering, emitting and absorbing properties has been studied and a detailed chemical kinetic mechanism has been used for combustion modeling. Also, the radiation heat flux from solid of porous media matrix to gas phase flow has been considered and is calculated with using the discrete ordinate method.

The main hypothesizes of this simulation are as follows:

1. The flow is turbulent and steady.
2. The burner is single layer.

3. The fluid flow is supposed as mixture of natural gas and air in the inlet with specified equivalence ration
4. The flow is supposed 1D.
5. The porous media is supposed homogeny.
6. The porous media is not in thermal equilibrium with gas flow.
7. The porous media is chemical inert.
8. Boundary conditions and the geometry considered here, adjustable with the experimental setup of Chaffin et al. [18].

Computational Domain

Figure 1 showing the computational domain considered here. The fuel and air enters to porous media as a premixed mixture at specified velocity and equivalence ratio. The total length considered for burner is 10.16 cm and is adjusted with experimental setup.

The porous media matrix properties are shown in tables 1.

Model Formulation

Governing equations of reactive fluid flow and combustion are continuity, momentum, species conservation and energy. These are one-dimensional, steady and turbulence flow and are obtained with

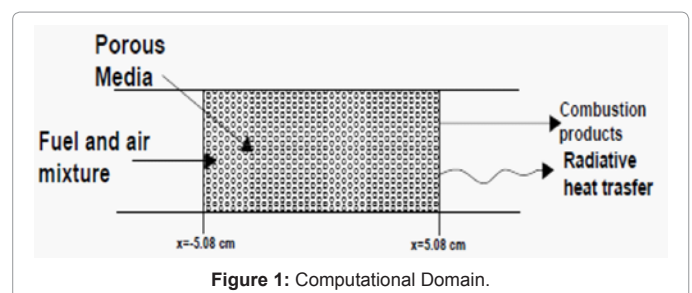


Figure 1: Computational Domain.

*Corresponding author: Bakhshan Y, Department of Mechanical Engineering, University of Hormozgan, PoBox 3990, Iran, E-mail: ybakhshan@yahoo.com

Received November 23, 2012; Published February 24, 2013

Citation: Bakhshan Y, Motadayen Aval S, Abdi B (2013) Turbulent Combustion Modeling Within Porous Media Using Detailed Chemical Kinetic. 2: 644 doi:[10.4172/scientificreports.644](http://dx.doi.org/10.4172/scientificreports.644)

Copyright: © 2013 Bakhshan Y, et al. This is an open-access article distributed under the terms of the Creative Commons Attribution License, which permits unrestricted use, distribution, and reproduction in any medium, provided the original author and source are credited.

using the space-time averaging as shown below.

Figure 2 showing, the symbols and method used for spaces-time averaging. The governing obtained equations are:

Continuity:

$$\nabla \cdot (\bar{u}_D) = 0 \tag{1}$$

Momentum:

$$\rho \nabla \cdot \left(\frac{\bar{u}_D \bar{u}_D}{\phi} \right) = - \left(\phi \langle \bar{p} \rangle^i \right) + \mu \nabla^2 \bar{u}_D + \nabla \cdot \left(-\rho \phi \langle u'u' \rangle^i \right) + \phi \rho g - \left[\frac{\mu \phi}{k} \bar{u}_D + \frac{CF \phi \rho / \bar{u}_D / \bar{u}_D}{\sqrt{k}} \right] \tag{2}$$

The superficial velocity is defined as below:

$$\bar{u}_D = \bar{u} \times \phi$$

For modeling of turbulence, the macroscopic K-ε model has been used as

$$\rho \nabla \cdot (\bar{u}_D \langle k \rangle) = \nabla \cdot \left[\left(\mu + \frac{\mu_t \phi}{\sigma K} \right) \nabla (\phi \langle k \rangle^i) \right] + C_k \rho \frac{\phi \langle k \rangle^i |\bar{u}_D|}{\sqrt{k}} - \rho \phi \langle \varepsilon \rangle^i$$

$$\rho \nabla \cdot (\bar{u}_D \langle \varepsilon \rangle) = \nabla \cdot \left[\left(\mu + \frac{\mu_t \phi}{\sigma K} \right) \nabla (\phi \langle \varepsilon \rangle^i) \right] + C_2 C_k \rho \frac{\phi \langle k \rangle^i |\bar{u}_D|}{\sqrt{k}} - C_2 \rho \phi \frac{\langle \varepsilon \rangle^i}{\langle k \rangle^i}$$

The turbulence viscosity and Reynolds stresses are obtained with using the Bossinque approximation as

$$\mu_{t\phi} = \rho C_\mu \frac{\langle K \rangle^i}{\langle \varepsilon \rangle^i}$$

$\beta = 270m^{-1}$	$\rho_s = 216m^{-1}$
$C_{p,s} = 824 J/kg.k$	$k_s = 1.6 W/m.k$
$\rho_s = 5.56 \times 10^3 kg/m^3$	$\phi = 0.87$ for 3.9 ppc

Table 1: Porous media properties.

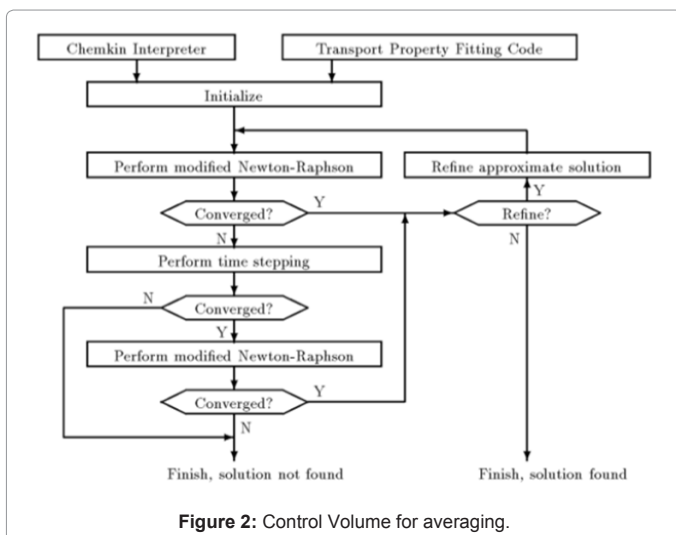


Figure 2: Control Volume for averaging.

$$-\rho \phi \langle u'u' \rangle^i = 2\mu_{t\phi} - \frac{2}{3} \phi \rho \langle k \rangle^i$$

$$\bar{u}_D = \bar{u} \times \phi \mu_{t\phi} = \rho C_\mu \frac{\langle k \rangle^i}{\langle \varepsilon \rangle^i}$$

Due to considering the non-equilibrium of porous material matrix (solid) with gas flow, the temperature of solid is different from gas flow. The energy equation of gas phase is

$$(\rho c_p)_f \nabla \cdot (u_D \langle \bar{T}_f \rangle^i) = \nabla \cdot (K_{eff,f} \nabla \langle \bar{T} \rangle^i) + h_i a_i (\langle \bar{T}_s \rangle^i - \langle \bar{T}_f \rangle^i)$$

and

$$K_{eff,f} = [\phi K_f + K_{disp} + K_{dispt}]$$

and

$$K_{disp} = \begin{cases} 0.022 \frac{\rho \varepsilon D^2}{(1-\phi)} \times K_f \text{ if } Pe_D < 10 \\ 2.7 \frac{Pe_D}{\phi^{0.5}} \times K_f \text{ if } Pe_D \geq 10 \end{cases}$$

$$Pe_D = Pe \times (1-\phi)^{1/2}$$

$$Pe = Re_p \times Pr$$

$$Re_p = \frac{U_d \times Pr}{\nu_f}$$

The energy equation of solid phase is

$$0 = \nabla \cdot (K_{eff,s} \nabla \langle \bar{T}_s \rangle^i) - \nabla q_{rad}$$

and

$$K_{eff,s} = (1-\phi)K_s$$

$$\nabla \cdot (\bar{u}_D \langle \bar{m}_{fu} \rangle^i) = \nabla \cdot D_{eff} \nabla (\phi \langle \bar{m}_{fu} \rangle^i) - \dot{\omega}_k k \varepsilon [1, N_s]$$

$$D_{eff} = D_{disp} + D_t + D_{disp,t} = D_{disp} + \frac{1}{\rho} \left(\frac{\mu \phi}{S_{cl,t}} + \frac{\mu_{t\phi}}{S_{cl,t}} \right) = D_{disp} + \left(\frac{\mu_{\phi,ef}}{S_{cl,ef}} \right)$$

The rate of species production in the combustion process can be found from mass conservation of species as below

$$\dot{\omega} = M_k \sum_{l=1}^N (v_{kl}^* - v_{kl}^i) K_l (\prod_{reactants} C^{v_{kl}} - \prod_{products} C^{v_{kl}})$$

and from Arrhenius equation we have

$$k_l = K_l^0 T^{\beta_l} \exp\left(-\frac{E_{l1}}{RT}\right)$$

Boundary Conditions

In this work, we used the boundary conditions at inlet and outlet for governing equations mentioned above. At inlet, specified inlet velocity, the energy balance, the energy balance with considering the radiation and the specified concentrations have been used for momentum, gas phase energy, solid phase energy and species equations respectively. At outlet, the constant phase temperature, balance energy with considering the radiation effect and the constant concentration of combustion products have been used. For turbulence kinetic energy and dissipation the following values have been used:

$$k_{in} = \frac{3}{2} I^2 u_{Din}^2, \varepsilon_{in} = K_{in}^2 \frac{\partial k_{out}}{\partial x} = 0, \frac{\partial \varepsilon_{out}}{\partial x} = 0$$

The boundary conditions used are summarized in table 2.

Results and Discussions

The governing equations mentioned above have been solved with implementation of finite difference method in one dimension with boundary conditions summarized in table 2. The calculation is started

with coarse grids and obtained solution is used as initial guess to main calculation with fined grids. The prepared computational algorithm is continued until the solution is converged. The flowchart of solution procedure is shown in figure 3.

The variation of gas temperature throughout the burner axial shown in figure 4. The onset of combustion location shows, the preliminary zone of burner plays as preheat zone and the chemical reactions started after this zone. The independency of solution from number of generated nodes has been shown in this figure also. Figure 5 shows the temperature variation for two different inlet velocities. These velocities are in the range of turbulence flow regime. With increasing velocity, onset of combustion delays in the axial of burner and this is due to increasing the inlet momentum of gas flow.

The variation of axial temperature at different equivalence ratios is shown in figure 6. The results show, the equivalence ratio of mixture for onset of combustion in the burner has a limit value and it is about 0.6

Inlet	Outlet
$u = u_{in}$	-----
$\dot{m} c_{ps} (T_{gi} - T_g) = -K_s \frac{dT_g}{dx}$	$\frac{dT_g}{dx} = 0$
$\dot{m} c_{ps} (T_{gi} - T_g) + \sigma \varepsilon (T_{surround}^4 - T_g^4) = -K_s \frac{dT_g}{dx}$	$H_v (T_{g,out} - T_g) + \sigma \varepsilon_{out} (T_{surround}^4 - T_g^4) = -k_s \frac{dT_g}{dx}$
$Y = Y_{in}$	$\frac{dY}{dx} = 0$

Table 2: Used boundary conditions.

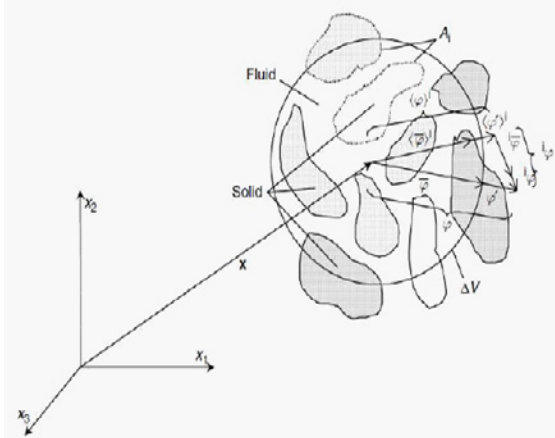


Figure 3: Flowchart of numerical solution.

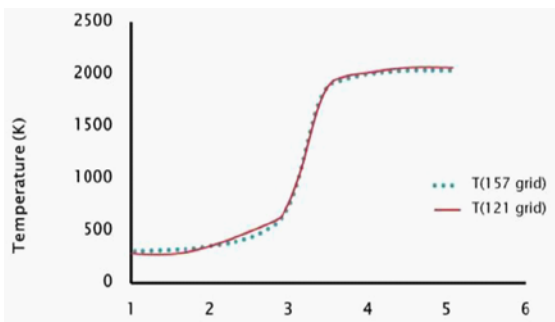


Figure 4: Axial Temperature Variation in the burner.

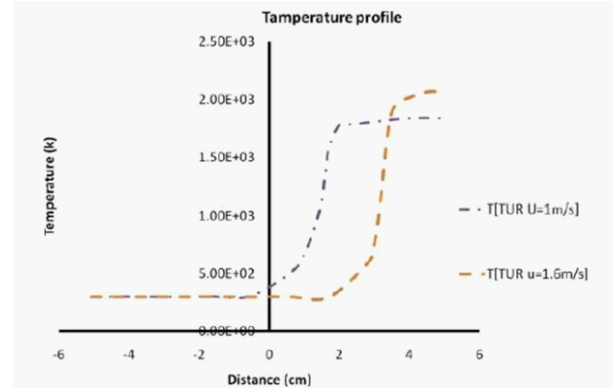


Figure 5: Temperature Variation at different inlet velocities.

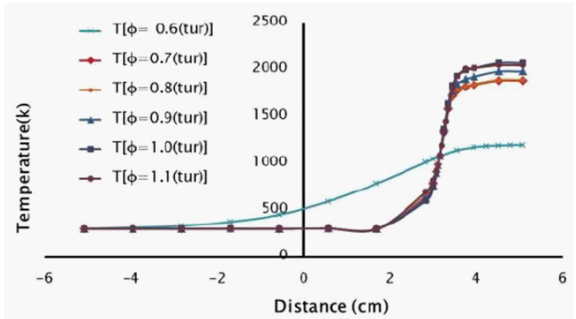


Figure 6: Temperature Variation at different equivalence ratios.

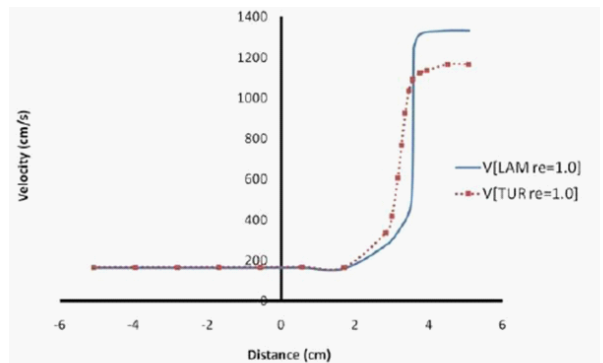


Figure 7: Velocity Profile throughout the burner.

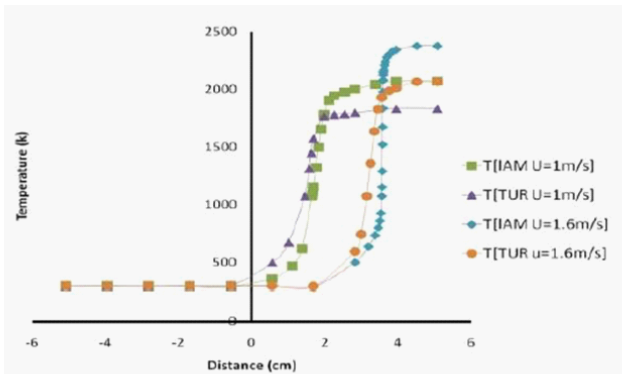


Figure 8: Temperature Variation at different velocities.

for the burner specified here. Under this value the combustion did not started and has not been stabilized the flame [19]. Using the laminar regime equations causes some errors in the results. The comparing of results is shown in figure 7. Figure 7 shows the velocity variation throughout the burner. The inlet velocity is same for two cases. Figure 8 shows temperature variation at different velocity and regimes. The results show onset of combustion in the turbulence mode delays in axial of the burner but its maximum value is higher at turbulence mode.

Figure 9 showing the variation of Reynolds number of flow throughout burner. With considering turbulence flow regime range, decreasing of inlet velocity causes, the flow regime change from turbulence to laminar in some places of burner and thus, the predicted results using the laminar equations have errors which it can be seen in figure 10.

Figure 10 showing the variation of NO which has high dependency on temperature versus the equivalence ratio. Because the used velocity is in the range of turbulence regime, the results for laminar flow regime have high deviation from experimental data. Also the results, showing the derived governing equations for turbulence regime in the porous burner in this research have acceptable agreement with experimental data and can be used in other works [20].

Figure 11 showing the variation of NO at different equivalence ratios throughout the burner. Increasing of equivalence ratio will increase the NO, and it takes maximum value at the stoichiometric point condition approximately. Onset of combustion and thus increasing the NO mole fraction after preheat zone of burner can be seen from this figure. The variation of carbon mono-oxide with equivalence ratio is shown in figure 12. With increasing the equivalence ratio, the CO mole fraction increases and this is due to increasing of fuel mass. Also the validation

of simulation results with experimental data can be seen from this figure.

The CO mole fraction variation throughout the burner at different equivalence ratios is shown in figure 13. Increasing the equivalence ratio, results the increasing of CO mole fraction, but its values froze at the end of burner.

Conclusion

In this study a numerical simulation of turbulent reactive flow in a porous burner is carried out. The fuel considered here is natural gas and a detailed chemical kinetic scheme is used for combustion modeling. The radiation heat transfer rate from solid phase to gas flow is considered. The simulation of turbulent is carried out for laminar regime and results are showing that using laminar regime equations in the burner have more deviation from experimental results. The simulated results at the turbulence regime flow are showing to have a good agreement with experimental values.

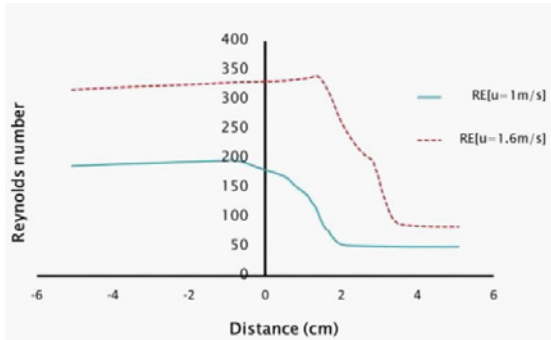


Figure 9: Reynolds number variation throughout burner.

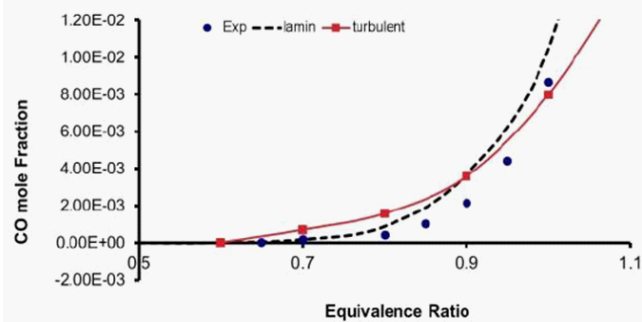


Figure 12: CO Variation versus equivalence ratio.

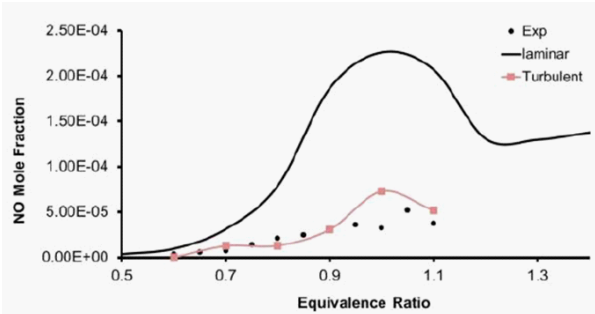


Figure 10: NO Variation versus equivalence ratios.

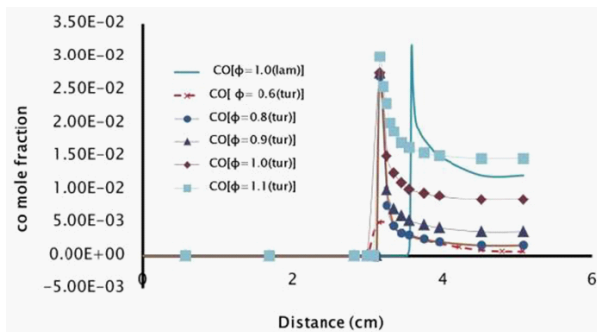


Figure 13: CO Variation throughout burner at different equivalence ratios.

References

1. Howell JR, Hall MJ, Ellzey JL (1996) Combustion of hydrocarbon fuels within porous inert media. *Prog Energ Combust* 22: 121-145.
2. Oliveira AAM, Kaviany M (2001) Non Equilibrium in the Transport of Heat and Reactants in Combustion in Porous Media. *Progress in Energy and Combustion Science* 27: 523-545.
3. Henneke MR, Ellzey JL (1999) Modeling of filtration combustion in a packed bed. *Combust Flame* 117: 832-840.
4. Bouma PH, De Goey LPH (1999) Premixed combustion on ceramic foam burners. *Combust Flame* 119: 133-143.
5. Babkin VS (1993) Filtrational Combustion of Gases - Present State of Affairs and Prospects. *Pure App Chem* 65: 335-344.
6. Leonardi SA, Viskanta R, Gore JP (2003) Analytical and experimental study of combustion and heat transfer in submerged flame metal fiber burners/heaters. *J Heat Trans* 125: 118-125.
7. Lammers FA, De Goey LPH (2003) A numerical study of flash back of laminar premixed flames in ceramic-foam surface burners. *Combust Flame* 133: 47-61.
8. Mohammad AA, Ramadhyani S, Viskanta R (1994) Modeling of combustion and heat transfer in a packed-bed with embedded coolant tubes. *Int J Heat Mass Trans* 37: 1181-1191.
9. Wood S, Harries AT (2008) Porous burners for lean-burn applications. *Prog Energ Combust Sci* 24: 667-684.
10. Hsu PF, Howell JR, Matthews RD (1993) A numerical investigation of premixed combustion within porous inert media. *J Heat Trans* 115: 744-750.
11. Lim IG, Matthews RD (1993) Development of a Model for Turbulent Combustion within Porous Inert Media. *Int J Fluid Mech Res* 25: 111-112.
12. Jones WP, Launder BE (1972) The prediction of laminarization with a two-equation model of turbulence. *Int J Heat Mass Trans* 15: 301-314.
13. Sahraoui M, Kaviany L (1995) Direct simulation vs volume-averaged treatment of adiabatic, premixed flame in a porous medium. *Int J Heat Mass Trans* 18: 2817-2834.
14. De Lemos MJS, Silva RA (2006) Turbulent flow over a layer of a highly permeable medium simulated with a diffusion-jump model for the interface. *Int J Heat Mass Trans* 49: 546-556.
15. Pedras MHJ, De Lemos MJS (2003) Computation of turbulent flow in porous media using a low-Reynolds k - ϵ model and an infinite array of transversally displaced elliptic rods. *Num Heat Trans Part A-App* 43: 585-602.
16. De Lemos MJS (2006) *Turbulence in Porous Media: Modeling and Applications*. Else Amsterdam 384.
17. De Lemos MJS (1995) Numerical simulation of turbulent combustion in porous materials. *Int J Heat Mass Trans* 18: 2817-2834.
18. Chaffin KC, Koeroghlian M, Matthews M, Hall M, Nichols S, et al. (1991) *Proceeding of the ASME/JSME Thermal Engineering Joint Conference Spring AFRC Meeting, Hartford* 4: 219.
19. Kee R, Grcar J, Smooke M, Miller J (1998) A FORTERAN program for modeling steady laminar one dimensional premixed flame. *Tech Repot SAND*.
20. Grcar J (1992) The twopnt program for boundary value problems. *Technical Report SAND*.